Impact of Melt Phase Formation on the High-Temperature Behaviour of MgO–CMA–C Refractories

Th. Preisker, P. Gehre, Chr. G. Aneziris, Chr. Wöhrmeyer, Chr. Parr

Due to their excellent thermomechanical properties and corrosion resistance against aggressive steel/slag systems, carbon-bonded magnesia (MgO–C), alumina-magnesia (AMC), and magnesia-alumina (MAC) bricks are the dominating refractories for the lining of the side walls and bottom of steel ladles, basic oxygen furnaces, and electric arc furnaces. In order to further improve the properties to meet the requirements for even longer service life, highly reactive spinel-rich powder/aggregates (2,5 mass-%, 5 mass-%, and 7,5 mass-%) has been introduced in the composition consisting of common MgO-C in two different qualities with 3 mass-% C (after carbonisation), carbonised at 1400 °C. Melt phase formation is expected after carbonisation that could support the formation of a protective layer on the brick surface to protect the brick from slag penetration and the carbon from oxidation. Thus, the influence of this melt phase formation on the thermomechanical properties has been studied. Besides the thermomechanical properties CCS, HMOR, apparent porosity, and median pore diameter, the phase composition after carbonisation has been analysed.

1 Introduction

Refractories based on magnesium oxide and carbon (MgO–C), alumina-magnesia-carbon (AMC), and magnesia-alumina-carbon (MAC) are the dominating lining materials in steelmaking and refining plants, like basic oxygen furnaces, electric arc furnaces, and steel ladles, where they have to withstand aggressive steel/slag systems, high temperatures in the range of 1600–1750 °C, and thermal shock [1]. Recent investigation deal with another type of spinel- and carbon-containing refractories – the MgO–$MgAl_2O_4$–C bricks in which pre-reacted spinel is added instead of alumina. A derivative of these bricks are MgO–CMA–C refractories, which contain coarse- or fine-grained spinel-rich calcium magnesium aluminate (CMA). Industrial trial tests with MgO–C bricks containing CMA were carried out by Pagliosa et al. and Wöhrmeyer et al. in the metal line of a 205 t, 130 t, 120 t, and 70 t ladle in different steel shops, respectively [2, 3]. These tests revealed a significant increase of the corrosion and penetration resistance, less wear in the joints, a more homogeneous wear profile, and especially the formation of a protective slag layer. The formation of the protective slag layer is traced to the addition of calcium magnesium aluminate to MgO–C, which increases the alumina and lime content of the infiltrating slag leading to a reduced reactivity [4].

A previous study clarified the effect of the addition of 5 mass-% of two common magnesium aluminate spinel raw materials, their grain size as well as the carbonization temperature on the properties of MgO–C with carbon-content of 3 % [5]. However, despite the outstanding corrosion resistance, melt phase formation is likely to occur at operating temperature through the interaction of MgO and its impurities with the phases contained in the CMA. For this reason, the aim of this work is to identify the influence of different grain sizes and amounts of CMA, and different graded MgO raw materials on the thermomechanical properties like CCS, HMOR, phase composition, apparent porosity, and pore size distribution, to offer a ladle lining material with both, optimised corrosion resistance and thermomechanical properties, which will in sum extend the service life of the bricks.

Theresia Preisker, Patrick Gehre, Christos G. Aneziris
Institute of Ceramic, Glass and Construction Materials
Technical University Bergakademie Freiberg
09599 Freiberg
Germany

Christoph Wöhrmeyer, Christopher Parr
Imerys Aluminates
Paris, France

Corresponding author: *Patrick Gehre*
E-mail: patrick.gehre@ikgb.tu-freiberg.de

Keywords: refractories, ladle, MgO–C properties

Received: 10.07.2019
Accepted: 22.07.2019

Tab. 1 Composition of the samples containing MgO 98 and MgO 95, respectively

Raw Material [mass-%]	95/98MgO-CMA2.5Z-C	95/98MgO-CMA5Z-C	95/98MgO-CMA7.5Z-C	95/98MgO-CMA2.5K-C	95/98MgO-CMA5K-C	95/98MgO-CMA7.5K-C
MgO 2–4 mm	17,0	17,0	17,0	17,0	17,0	17,0
MgO 1–2 mm	24,7	24,7	24,7	27,2	24,7	22,2
MgO 0–1 mm	34,3	34,3	34,3	34,3	34,3	34,3
MgO powder	19,3	16,8	14,3	16,8	16,8	16,8
MagA –200	2,5	5,0	7,5	–	–	–
MagA –1/2	–	–	–	2,5	5,0	7,5
Graphite	1,1	1,1	1,1	1,1	1,1	1,1
Carbon black	1,1	1,1	1,1	1,1	1,1	1,1
Powder resin	1,5	1,5	1,5	1,5	1,5	1,5
Liquid resin	1,5	1,5	1,5	1,5	1,5	1,5
Hardener	0,3	0,3	0,3	0,3	0,3	0,3

2 Experimental

The raw materials used for the preparation of the MgO–CMA–C sample bodies were magnesium oxide with a purity of 95 and 98 % (CS 95 and SM 98, RHI Magnesita/AT), respectively, and calcium magnesium aluminate powder (–200 mesh) and aggregates (–1/2) (MagARMOUR, Imerys Aluminates/FR), respectively, in a range of 2,5–7,5 mass-%.

Tab. 1 shows the composition of the samples. MgO was used with varied fractions up to 4 mm particle size and the carbon content was adjusted to 2,2 mass-%, whereby graphite and carbon black were added in equal parts. MagARMOUR (in the following MagA) aggregates were sieved to a maximum grain size of 2 mm in order to replace parts of the MgO 1–2 mm fraction.

As the first mixing step, the coarse MgO fractions and MagA 1–2 mm were premixed for 3 min. Afterwards, the liquid resin 9308-FL (Hexion/DE), which was heated up to 70 °C in a temperature control was added and mixed for another 2 min. As the last step in the mixing process, fine MgO, MagA –200 mesh, graphite NFL, carbon black Thermaxx N991 (Luvomaxx/DE), powder resin 0235 DP (Hexion), and hexamethylenetetramine (Hexion) as hardener were added and mixed for another 5 min to achieve a homogeneous distribution of the raw materials in the mixture. After completing the mixing process of all batches, different test bodies were pressed. 5 bar-shaped samples (25 mm × 25 mm × 150 mm) per batch were pressed with a uniaxial press with an applied pressure of 120 MPa.

Furthermore, 6 cylinders per batch with 50 mm height and 50 mm diameter were pressed (RUCKS engine building GmbH/DE). Thermal treatment was applied to the samples after pressing by hardening in a three steps schedule with a maximum temperature of 180 °C. Afterwards, the samples were carbonised in SiC retorts filled with petrol coke for 5 h at a temperature of 1400 °C to provide a reducing atmosphere. For the XRF analysis of the raw materials, a wavelength-dispersive spectrometer type S8 Tiger (Bruker AXS GmbH/US) was used.

Tab. 2 Oxide composition determined by XRF

	SM 98 [mass-%]	CS 95 [mass-%]	MagA –200 [mass-%]
MgO	96,73	94,50	20,02
CaO	1,14	2,43	9,17
Al_2O_3	0,42	0,38	70,01
SiO_2	1,06	1,77	0,27
Fe_2O_3	0,52	0,74	0,11
Traces	0,13	0,18	0,42
Sum	100,00	100,00	100,00

The Cold Crushing Strength (CCS) was determined at cylinders according to DIN EN 993-5 with a 100 kN universal testing machine TiraTest 28100 (TIRA GmbH/DE). The Hot Modulus of Rupture (HMOR) was determined on bar-shaped sample bodies under argon atmosphere based on DIN EN 993-7 with an apparatus from Netzsch/DE. The final temperature of the HMOR was 1400 °C with a heating rate of 10 K/min and a soaking time of 30 min was applied for a homogenous temperature distribution before HMOR test.

The Apparent Porosity (AP) was determined with fragments after the CCS test by the so-called Archimedes' principle according to DIN EN 993-1 using toluol as intrusion medium. Furthermore, in order to obtain information on the pore size distribution, mercury intrusion method, as comprehensively explained in DIN 66133, was performed.

Thus, remaining fracture pieces of the CCS examination were measured with an assumed contact angle of 140° using a MicroActive AutoPore V 9600 1,03 (Micromeritics Instrument Corporation/US). Fragments of the CCS were also used for phase identification of the different batches by X-Ray Diffraction (XRD). The fragments were ground to a maximum grain size of 20 µm in a vibratory disc mill and finally analysed with the diffractometer X'Pert Pro MPD (Philips/NL) using a Cu Kα-radiation with Kα 1(Å) = 1,54060. Phase analysis was performed using the software X'Pert HighScore Plus.

3 Results and discussion

Although the MgO content in magnesia is important up to a certain level, the type of impurities and their ratio plays a vital role in achieving good performance. In order to analyse the used raw materials SM 98 (fused magnesia) and CS 95 (sintered magnesia) concerning their chemical composition, XRF analysis was performed and the results are compiled in Tab. 2. All magnesia raw materials possess the stated purity. CaO and SiO_2 are the main impurities in SM 98 and CS.

Another major impurity in both raw materials is Al_2O_3. Several traces like SO_3, Cl, K_2O, Mn, P_2O_5, Zn, and TiO_2 were found but they are of less importance because they have in total a proportion of less than 0,5 mass-%. The calculated C/S ratio is 1,075 for SM 98 and 1,373 for CS 95.

3.1 Phase composition – XRD

Tab. 3 gives an overview of all main phases as well as detectable traces of MgO–C with MagA addition after carbonisation at 1400 °C. All samples contain as main phases MgO, $MgAl_2O_4$, and C. The general trend is that the more MagA was used, the more spinel was detectable, which was verified by Rietveld analysis. The amount of CA-phases containing in MagA (CA and CA_2) decrease most likely due to the formation of additional spinel by reaction of Al_2O_3 of the CA-phases with MgO if the carbonisation temperature is high enough.

With respect to the use of CS 95 and SM 98 as MgO raw material, there are differences notable in the formed trace phases. Using CS 95 leads to the trace phases $Ca_{12}Al_{14}O_{33}$ (mayenite), Ca_2SiO_4 (calcium silicate), and an iron-containing phase, whereas samples with MagA aggregates showed $CaFeSi_2O_6$ (hedenbergite) as iron-containing phase and those with MagA powder $Ca_3Fe_2Si_3O_{12}$ (andradite). Similar to the samples containing CS 95, all samples where SM 98 was used contain as trace phase $Ca_{12}Al_{14}O_{33}$ (mayenite). In contrast to CS 95 samples, no iron-containing phases could be detected in samples containing SM 98, which could be traced to the higher purity of SM 98 determined by XRF analysis (less Fe_2O_3).

Thus, iron-containing phases are below the determination limit. Taking the influence of MagA powder in SM 98 into account, the formation of minor phases, which differ from those detected in samples containing MagA aggregates is observed. In samples containing MagA aggregates, only $Ca_{12}Al_{14}O_{33}$ (mayenite) could be detected, whereas $Ca_2MgSi_2O_7$ (akermanite) could be additionally detected using MagA powder.

Furthermore, the sample with the lowest MagA powder portion showed the formation of Mg_2SiO_4 (forsterite), which is an impurity in MgO and could be therefore clearly identified. To sum up, the iron-containing minor phases ($CaFeSi_2O_6$ and $Ca_3Fe_2Si_3O_{12}$, respectively), as well as akermanite are expected to be the melting phases, which will decrease the high-temperature properties.

Tab. 3 Main phases and detectable traces after carbonisation at 1400 °C

Sample	Main Phases	Traces
95MgO-CMA2.5K-C	MgO, $MgAl_2O_4$, C	$Ca_{12}Al_{14}O_{33}$, Ca_2SiO_4, $CaFeSi_2O_6$
95MgO-CMA5K-C	MgO, $MgAl_2O_4$, C	$Ca_{12}Al_{14}O_{33}$, Ca_2SiO_4, $CaFeSi_2O_6$
95MgO-CMA7.5K-C	MgO, $MgAl_2O_4$, C	$Ca_{12}Al_{14}O_{33}$, Ca_2SiO_4, $CaFeSi_2O_6$
95MgO-CMA2.5Z-C	MgO, $MgAl_2O_4$, C	$Ca_{12}Al_{14}O_{33}$, $Ca_2MgSi_2O_7$, $Ca_3Fe_2Si_3O_{12}$
95MgO-CMA5Z-C	MgO, $MgAl_2O_4$, C	$Ca_{12}Al_{14}O_{33}$, $Ca_2MgSi_2O_7$, $Ca_3Fe_2Si_3O_{12}$
95MgO-CMA7.5Z-C	MgO, $MgAl_2O_4$, C	$Ca_{12}Al_{14}O_{33}$, $Ca_2MgSi_2O_7$, $Ca_3Fe_2Si_3O_{12}$
98MgO-CMA2.5K-C	MgO, $MgAl_2O_4$, C	$Ca_{12}Al_{14}O_{33}$
98MgO-CMA5K-C	MgO, $MgAl_2O_4$, C	$Ca_{12}Al_{14}O_{33}$
98MgO-CMA7.5K-C	MgO, $MgAl_2O_4$, C	$Ca_{12}Al_{14}O_{33}$
98MgO-CMA2.5Z-C	MgO, $MgAl_2O_4$, C	$Ca_{12}Al_{14}O_{33}$, $Ca_2MgSi_2O_7$, Mg_2SiO_4
98MgO-CMA5Z-C	MgO, $MgAl_2O_4$, C	$Ca_{12}Al_{14}O_{33}$, $Ca_2MgSi_2O_7$
98MgO-CMA7.5Z-C	MgO, $MgAl_2O_4$, C	$Ca_{12}Al_{14}O_{33}$, $Ca_2MgSi_2O_7$

3.2 Cold Crushing Strength – CCS

Fig. 1 shows the results of the determination of the cold crushing strength of the samples containing different MgO raw materials (SM 98 and CS 95) and different amounts (2,5 mass-%, 5 mass-%, and 7,5 mass-%) of MagA (powder and aggregates).

The highest CCS show the samples containing MgO 95 with MagA powder, whereby the maximum CCS (35,88 MPa) was measured at the sample with the lowest MagA powder content (2,5 mass-%). The CCS slightly decreases with rising MagA content for the MgO/MagA powder samples. Similar results were obtained with MgO 98 and MagA powder.

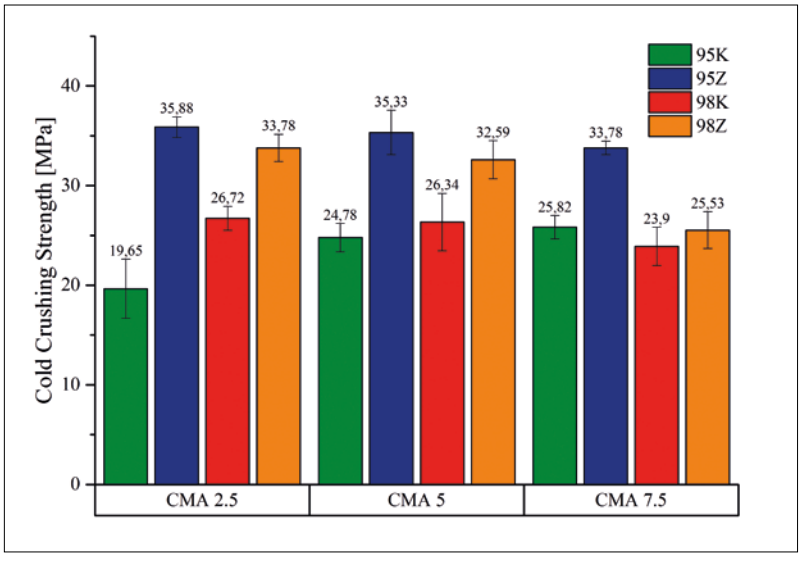

Fig. 1 CCS of samples containing SM 98 and CS 95, respectively, as well as MagA aggregates and powder, respectively

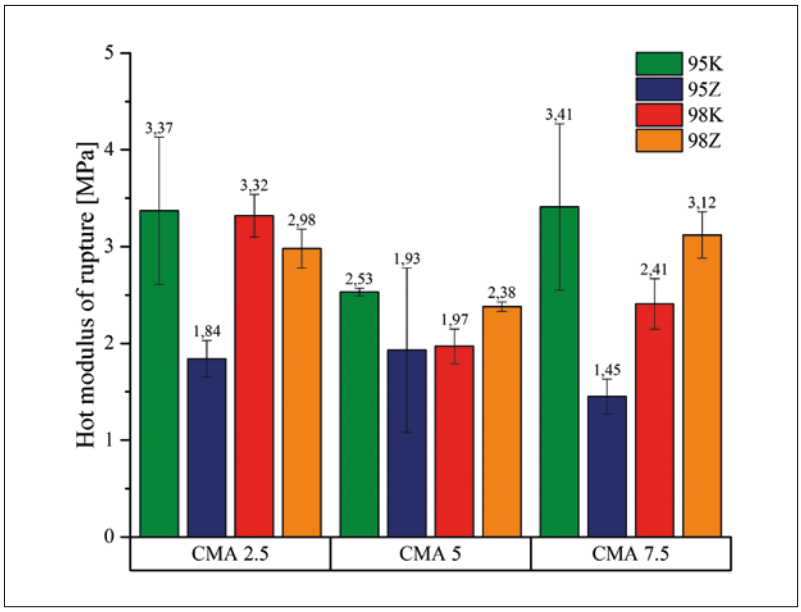

Fig. 2 HMOR of samples containing SM 98 and CS 95, respectively, as well as MagA aggregates and powder, respectively

In this case, the maximum CCS is 33,78 MPa, which belongs as well to the sample with the lowest amount of MagA powder. Using higher portions of MagA leads to a decrease in CCS. In general, the use of MagA aggregates is evaluated as negatively in comparison to the use of MagA powder. All determined values of the samples containing MagA aggregates are below the belonging compositions with MagA powder. For MgO 95 and MagA aggregates, the CCS increases with higher amounts of MagA aggregates.

In contrast, CCS values of MgO 98 with MagA aggregates decrease with rising amount of MagA. The CCS of the sample 95 MgO-CMA2.5 K-C is the lowest by far with a CCS of 19,65 MPa. Of cause, differences in CCS might also be attributed to differences in compact ability of the mixes linked to deviant particle size distribution resulting in different pressing density.

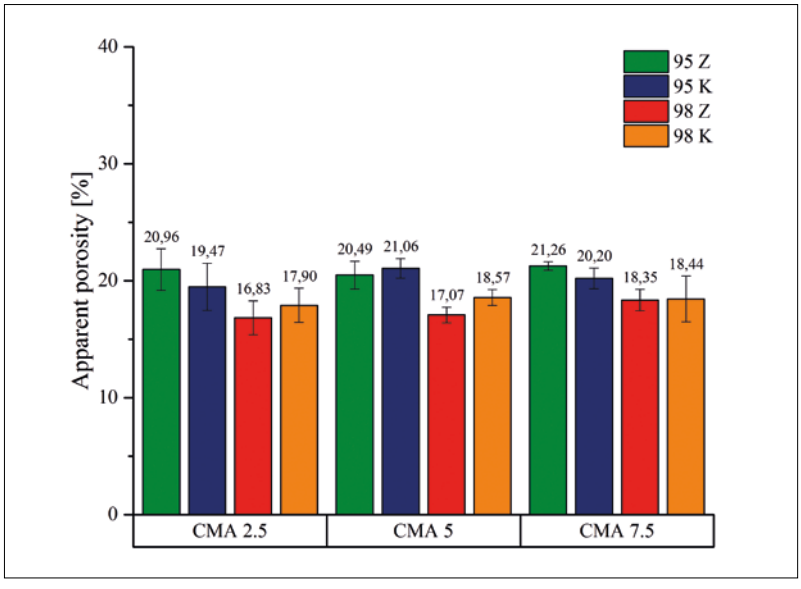

Fig. 3 Apparent porosity of samples containing SM 98 and CS 95, respectively, as well as MagA aggregates and powder, respectively

3.3 Hot Modulus of Rupture – HMOR

Fig. 2 displays the average HMOR values at 1400 °C of samples containing SM 98 and CS 95, respectively, as well as MagA aggregates and powder, respectively, with varying MagA content. In general, the HMOR values of the sample bodies do not show an expected change of strength. Although the samples MgO 95 with MagA aggregates exhibit the lowest CCS of the testes sample bodies, they show the best results at HMOR. Sample 95 MgO-CMA 7,5K-C possess the highest measured HMOR with a value of 3,41 MPa. In contrast, sample 95 MgO-CMA 7,5 Z-C distinctly lose strength at the applied temperature of 1400 °C (lowest value: 1,45 MPa with MagA 7,5 mass-%), whereas these samples showed the highest CCS of all measured samples.

Reasons for this are nearly full decarbonisation during the test run, even by constant argon flow, leading to loss of the binding structure (carbon network). The high standard deviation supports this assumption. Consequently, it is not evident, which MagA content is advisable for achieving a HMOR as high as possible but using MgO 98 together with MagA shows a minimum HMOR with 5 mass-% MagA powder and aggregates, respectively. Additionally, the samples containing MgO 98 exhibit a higher HMOR as the samples containing MgO 95 with MagA powder.

3.4 Apparent porosity and pore size distribution

Next to strength, Apparent Porosity (AP) and pore size distribution are crucial properties of refractories. Open pores highly influence the slag infiltration and corrosion behaviour. In general, a low apparent porosity reduces the penetration of slag and probably improves the oxidation resistance. A higher AP could influence the thermal shock resistance in a positive way as well. The values of the apparent porosity of the samples containing SM 98 and CS 95, respectively, as well as MagA aggregates and powder, respectively, after carbonisation at 1400 °C are given in Fig. 3. Furthermore, the d_{50} values of all samples as a result of the mercury intrusion method are compiled in Fig. 4.

Generally, the apparent porosities of the tested sample fragments do not vary tremendously, so they are in a range of 16,8 %

to 21,3 %. Also for the apparent porosity, there seems to be no clear dependence of the MagA content. The lowest apparent porosities were obtained in samples containing MgO 98 in combination with MagA powder. In contrast, the highest average apparent porosities were achieved with samples MgO 95/MagA powder and MgO 95/MagA aggregates.

The d_{50} value is of great importance as well, since the pore size influences the infiltration of liquids. The critical pore size to prevent infiltration by steel is known to be approx. 30 µm. The d_{50} pore size values of all samples (Fig. 4) fulfil this requirement.

However, the critical pore size of slag infiltration can be much lower depending on the slag chemistry.

Additionally, the samples may contain several bigger pores, which will cause steel and slag infiltration though. The measured portion of pores >30 µm is between 9 % (95 MgO-CMA5Z-C) and 22 % (98 MgO-CMA 7,5 K-C). The lowest d_{50} value (3,91 µm) was achieved by the sample 95 MgO-CMA 5 Z-C and the highest by the sample 98 MgO-CMA 7,5 K-C (10,89 µm).

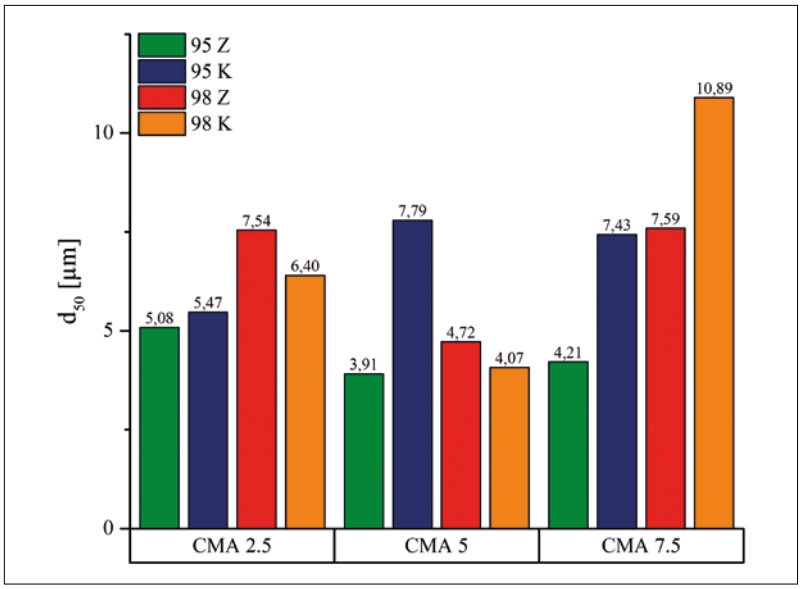

Fig. 4 The d_{50} value of samples containing SM 98 and CS 95, respectively, as well as MagA aggregates and powder, respectively

4 Conclusion

The influence of the introduction of the calcium magnesium aluminate MagA to MgO–C bricks on the thermomechanical properties cold crushing strength, hot modulus of rupture, apparent porosity, median pore diameter, and the phase composition after carbonisation have been analysed.

The aim of the study was to clarify the effect of the addition of two different grades of MgO raw material and varied amounts of MagA (2,5 mass-%, 5 mass-%, 7,5 mass-%).

After carbonisation, changes in phase composition depending on the used MgO raw materials and MagA (powder and aggregates) are detected.

Using CS 95, iron-containing phases are detected as trace phases, resulting from the impurities in the raw material. Using MagA, especially in the form of powder leads to an increased CCS.

However, the determined values of the HMOR, although generally relatively low, didn't show the same trend and surprisingly did not show a decrease with increasing MagA content. Apparent porosity is in the range of 16,8–21,3 %, whereby no clear dependence on the MagA content could be figured out.

SM 98 slightly decreases the apparent porosity. All measured d_{50} values are below the critical value for steel melts (30 µm), whereby the sample with CS 95 and 5 mass-% MagA powder displayed with 3,91 µm the lowest median pore diameter.

References

[1] Figueiredo Jr., A.; et al.: Technological evolution of magnesia-carbon bricks for steel ladles in Argentina. Iron and Steel Technology (2004) [1] 42–47

[2] Pagliosa, C.; Souza, P. V.; Hama, N.: Improvement of MAC bricks for steel ladle with CaO-MgO-Al_2O_3 aggregate: A new perspective for cement application. Proc. UNITECR 2017, Santiago de Chile, 2017, 169–172

[3] Wöhrmeyer, Chr.; et al.: Protection mechanism of CMA-additives in MgO–C ladle bricks. Proc. 61th Int. Colloquium on Refractories, Aachen, 2018, 54–59

[4] Gehre, P.; et al.: Untersuchung der Schutzwirkung von MgO-C-Pfannensteinen mit CMA-Zusatz. Keram. Z. **70** (2018) 40–46

[5] Gehre, P.; et al.: Functional Spinel-Binder Based Additives for Improved MgO–C Performance in Ladle Applications. refractories WORLDFORUM **9** (2017) [3] 83–88